AACL BIOFLUX
Aquaculture, Aquarium, Conservation & Legislation
International Journal of the Bioflux Society

Numerical investigation of velocity profiles in the lateral intakes using finite-volume method and comparison with experimental results in water distribution networks

[1]Adel A. Ashari, [1]Edris Merufinia, [2]Ebrahim Nohani

[1] Young Researchers and Elite Club, Mahabad Branch, Islamic Azad University, Mahabad, Iran; [2] Department of Hydraulic Structures, Dezful Branch, Islamic Azad University, Dezful, Iran. Corresponding author: E. Nohani, nohani_e@yahoo.com

Abstract. Intakes are generally used in water distribution networks, irrigation channels, sewage networks, water/wastewater treatment facilities, input to power generation facilities, etc. Due to the flow complexity and also the effects of scale, physical models can not solely provide a clear understanding of the physics governing the flow field and it is necessary to study this phenomenon numerically along with field and experimental studies. At the first of this study, the flow numerical simulation has been performed in the direct path of rectangular channel and Navier-Stokes equations are solved by Finite-Volume Method (FVM). The flow calculations were performed in the three dimensional model using K-ε-RNG and K-ε-standard turbulence models. The K-ε-Standard turbulence model showed the best results according to the comparison of velocity profiles with the experimental results of Barkdoll et al (1998), and the results of other numerical studies. Then, using this turbulence model, the flow velocity profiles at different sections of the main channel and intake were compared with the experimental and numerical results of other researchers, and a good agreement has been found between them. The comparison of the obtained results with experimental and numerical results of other researchers indicates that this numerical model can well predict the flow velocity profile in different sections of the main channel and intake.

Key Words: lateral intake, flow velocity profile, shear stress and pressure distribution, Finite-Volume Method, turbulence models.

Introduction. Water has been diverted from its original pathway since a long time ago for a variety of applications, including agriculture, urban water supply, etc. Rivers are one of the cheapest and most available water resources for irrigation of green areas and agriculture, including fish farming which impoundment for different applications is important. The flow diverted into the intake has complex specifications and leads to the creation of flow separation zones in the main channel and intake (Safarzadeh & Salehi Nishabouri 2004). In this area of flow, fluid particles in the vicinity of the left wall of intake channel (toward the entry of the main channel) are rotational and actually this area of the lateral channel will have no effect on flow discharge rate. Due to the changes in velocity distribution in the intake area, sedimentation usually occurs at the intake entrance, which leads to the reduction in intake efficiency, entry of coarse sediments into the network and the increase in administrative costs for sediment removal operations. Every step which leads to the reduction in the secondary and vortex flows at intake entrance, will lead to the reduction in sediment accumulation at intake entrance as well as reduction in the sediment entering in to the intake. Law & Reynolds (1966) performed an analytical and experimental study on the main channel and deviation with equal width and succeeded to present a relation for the ratio of discharges, Froude number before and after the junction, and the ratio of widths of the two channels. Chen & Lian (1992), two-dimensionally simulated the geometry of T-junction, which was studied experimentally by Popp & Sallet in 1983, using standard K-ε model with above Reynolds

numbers. The results obtained for the ratio of small discharges had proper agreement with the previous experimental measurements, but in the bigger discharges ratio, their predictions were significantly different with the measurements. Neary & Odgaard (1993) performed experimental studies on the flow hydraulics at 90 degree intakes. In this study, flow pattern, flow separation line, rest area, and the vortex formation area were investigated and the power of rotational flow in the vortex formation area increased with increasing the ratio of velocity in the intake channel to the main channel. Hager (1987), performed experimental studies on the measurement of length and width of the flow rotation area at 90 degree intake of a rectangular channel, and concluded that the dimensions of the flow separation zone depend on the ratio of diverted discharge and length and width of the rotation area at intake channel entrance decrease with increasing the intake ratio. Ramamurthy et al (2007) performed experimental studies at 90 degree intake for an open channel of rectangular section and used three-dimensional precise instrumentations to measure velocity at different sections. Issa & Oliveira (1994) performed three-dimensional simulation of turbulent flow for T-shaped geometries. They solved Reynolds time-averaged Navier–Stokes equations (RANS) through K-ε-Standard model with wall functions. In their research, the equations were solved using Finite-Volume Method (FVM) with accuracy of one-order. Neary et al (1996) surveyed the layer flow pattern at 90 degree intake by providing a three-dimensional numerical model. These researchers used Finite-Volume method for solving the equations and managed to examine flow pattern in this field and qualitatively simulate the movement of bed load sediment particles. Neary et al (1999) performed a parametric study on the flow pattern in the lateral intake three-dimensionally using K-ω turbulence model. Shamloo & Pirzadeh (2008), numerically simulated flow hydraulics in the river lateral intakes using the Fluent Software. In this research, by choosing K-ε-Standard turbulence model, flow velocity profiles were evaluated three-dimensionally and a good agreement has been found between the obtained values and the experimental results. Goudarzizadeh et al (2010) numerically investigated a three-dimensional examination of the flow pattern in the intake in the direct path using the Finite Volume method.

The aim of this study is to compare K-ε-RNG turbulence model, flow velocity profiles at different sections of the main channel and intake with the experimental results.

Numerical model and the governing equations. In this study, Navier-Stokes equations are solved by three-dimensional Finite-Volume Method (FVM). FVM is based on direct discretization of the integral form of conservation laws in physical space. Flow analysis occurs at persistent mode and simple algorithm uses for velocity-pressure coupling. Several number of turbulence models exist in this numerical model. Method of discritization of momentum equation, loss and turbulence kinetic energy and Reynolds stress is two-order leading method. Also, standard method is use for discritization of pressure equation.

Considering the differential form of conservation law (equation 1), the important step in the FVM is integral form of the governing equations over the control volume.

Equation (1) $$\frac{\partial U}{\partial t}+\vec{\nabla}\cdot\vec{F}=Q$$

Equation (2) $$\int_{\Omega_J}\frac{\partial U}{\partial t}d\Omega+\int_{\Omega_J}\vec{\nabla}\cdot\vec{F}d\Omega=\int_{\Omega_J}Qd\Omega$$

Using Gauss' divergence theorem,

Equation (3) $$\int_{\Omega_J}\vec{\nabla}\cdot\vec{F}d\Omega=\int_{S}\vec{F}\cdot d\vec{S}$$

The integrated form of conservation law for each control volume Ω_j related to the point j will be as follows:

Equation (4) $$\frac{\partial}{\partial t}\int_{\Omega_J} U d\Omega + \int_{S_J} \vec{F}\cdot d\vec{S} = \int_{\Omega_J} Q d\Omega$$

The above equation is replaced by its discrete form in which the integral volume is expressed as averaged values on the cell and the integral surface as the total volume.

Equation (5) $$\frac{\partial}{\partial t}\left(U_J \Omega_J\right) + \sum_{faces} \vec{F}\cdot \Delta\vec{S} = Q_J \Omega_J$$

Where, U is flow velocity, F is force, Q is flow discharge and Ω_j is control volume related to the point j. Equations 6 and 7 are 3D continuity and momentum equations for turbulent flow in the incompressible fluid, respectively. Also, in different turbulence models, the turbulence kinetic energy is also defined according to the equation 8 (Olsen 2006).

Equation (6) $$\frac{\partial \overline{U_i}}{\partial x_i} = 0$$

Equation (7) $$\frac{\partial \overline{U}i}{\partial t} + (\overline{U_j})\frac{\partial \overline{U_i}}{\partial x_j} = -\frac{1}{\rho}\frac{\partial \overline{p}}{\partial x_i} + g_{xi} + \frac{\partial}{\partial x_j}[\nu \frac{\partial \overline{U}i}{\partial x_j} - \overline{U_i' U_j'}]$$

Equation (8) $$K = \frac{1}{2}\overline{U_i U_i}$$

Where, $\overline{U_i}$ and $\overline{U_j}$ are flow velocity in x and y directions, respectively, t is time, v is molecular viscosity, p is pressure, k is turbulence kinetic energy, ρ is fluid density and g_{xi} is gravity acceleration in the x_i direction.
In k-ε turbulence model, turbulence kinetic energy (k) is modeled as follows:

Equation (9) $$\frac{\partial k}{\partial t} + U_j \frac{\partial k}{\partial x_i} = \frac{\partial}{\partial x_j}(\frac{\nu_T \partial k}{\sigma_k \partial x_j}) + p_k - \varepsilon$$

P_k is defined as follows:

Equation (10) $$P_k = \nu_T \frac{\partial U_j}{\partial x_i}(\frac{\partial U_j}{\partial x_i} + \frac{\partial U_i}{\partial x_j})$$

Equation (11) $$\nu_T = c_\mu \frac{K}{\varepsilon^2}$$

The dissipation of k is denoted ε as follows:

Equation (12) $$\frac{\partial \varepsilon}{\partial t} + U_j \frac{\partial \varepsilon}{\partial x_j} = \frac{\partial}{\partial x_j}(\frac{\nu_T \partial \varepsilon}{\sigma_k \partial x_j}) + C_{\varepsilon 1}\frac{\varepsilon}{k}P_k + C_{\varepsilon 2}\frac{\varepsilon^2}{k}$$

In the above equations, s is stress tensor, P_k is the term of turbulence production and experimental constant values used are as follows (Olsen 2006).

Equation (13) $$C_\mu = 0.09,\ C_{1\varepsilon} = 1.43,\ C_{2\varepsilon} = 1.92,\ \sigma_\varepsilon = 1.3,\ \sigma_k = 1$$

Characteristics of the experimental model of Barkdoll et al (1998). In the experimental study of Barkdoll et al (1998), the main channel with length of 2.74 m and the intake channel with length of 1.68 m located at 90° have been investigated. The discharge entered into the main channel (Q_1) is 11 L/s, ratio of diverted discharge (R) is 0.31, depth of flow (d) is 0.31 m, Reynolds number (Re) is 49600 and width of both channels (b) is 0.152 m. Figure 1 shows a schematic of the channel and hydraulic characteristics of water flow are given in Table 1.

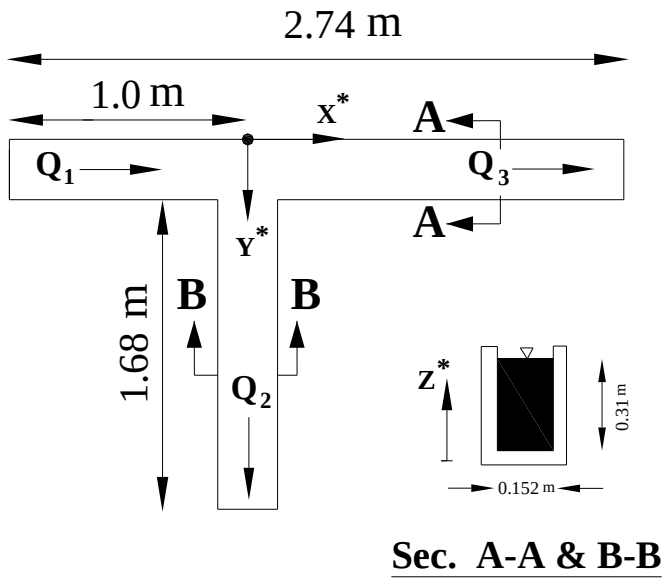

Figure 1. Geometric characteristics of laboratory flume.

Table 1

Hydraulic characteristics of flow

d (m)	*Q_1 (L/s)*	*R*	*Q_3 (L/s)*	*Q_2 (L/s)*	*Re*	*Fr*
0.31	11	0.31	7.59	3.41	49600	0.13

Meshing and boundary conditions of the computational domain. In this study, the main channel entrance uses the boundary condition of a given velocity with the average velocity of 0.244 m/s. Ratio of diverted discharge (R) is 0.31 according to the amount considered in the experimental model. Considering the small changes in water level, the symmetry boundary condition is applied to the water level. The rigid boundary and no-slip conditions are applied for wall. Appropriate meshing of regional which flow exists is also one of the important parameters in the model run time. Figure 2 shows the three-dimensional plan and view of computational domain meshing in the 90 degree intake. The number and dimensions of cells in its different areas in the x, y and z directions are given in Table 2.

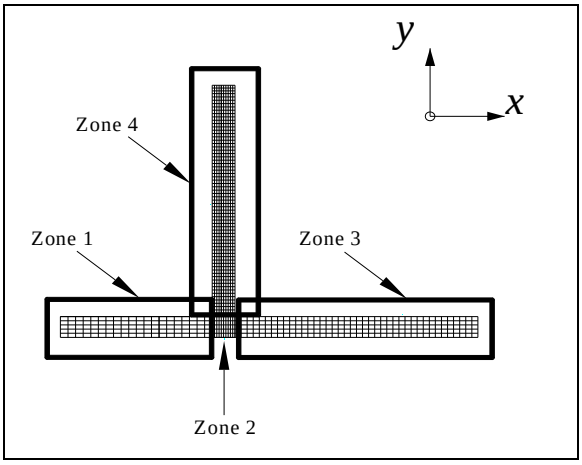

)a(

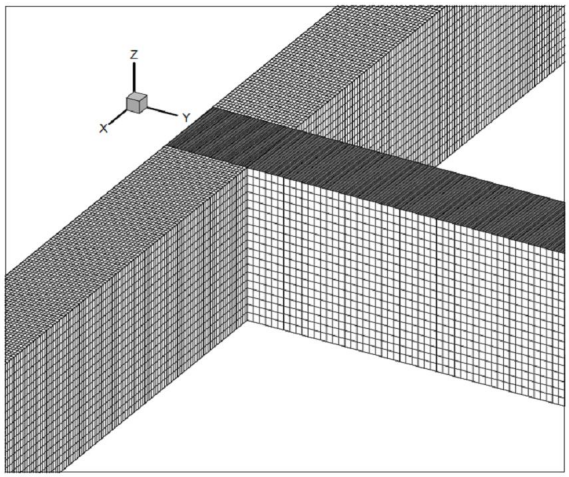

)b(

Figure 2. Computational mesh which is used in simulation, a) plan and b) three-dimensional view.

Table 2

The number and dimensions of cells in computational domain grid areas at different directions

	No. of cells at x direction	*No. of cells at y direction*	*No. of cells at z direction*	*Cell dimensions at x direction (mm)*	*Cell dimensions at y direction (mm)*	*Cell dimensions at z direction (mm)*
Zone 1	120.00	24.00	19.00	7.70	6.25	16.31
Zone 2	50.00	24.00	19.00	3.00	6.25	16.31
Zone 3	240.00	24.00	19.00	6.98	6.25	16.31
Zone 4	50.00	150.00	19.00	3.00	11.20	16.31

Evaluation of flow velocity profiles. In Figure 3, according to the experimental study, the dimensionless velocity profiles (U_x/U_0) near the water level, for different cross-sections of the main channel for entrance constant discharge of 11 L/s, the ratio of diverted discharge (R) and the Froude number of entrance flow (Fr) are shown 0.31 and 0.13, respectively. X^* and Y^* are distances at x and y axes, respectively which have become dimensionless by width of intake channel (b). U_0 is the maximum velocity at the cross-section X^*=-4.65 whose value is equal to 0.28 m/s.

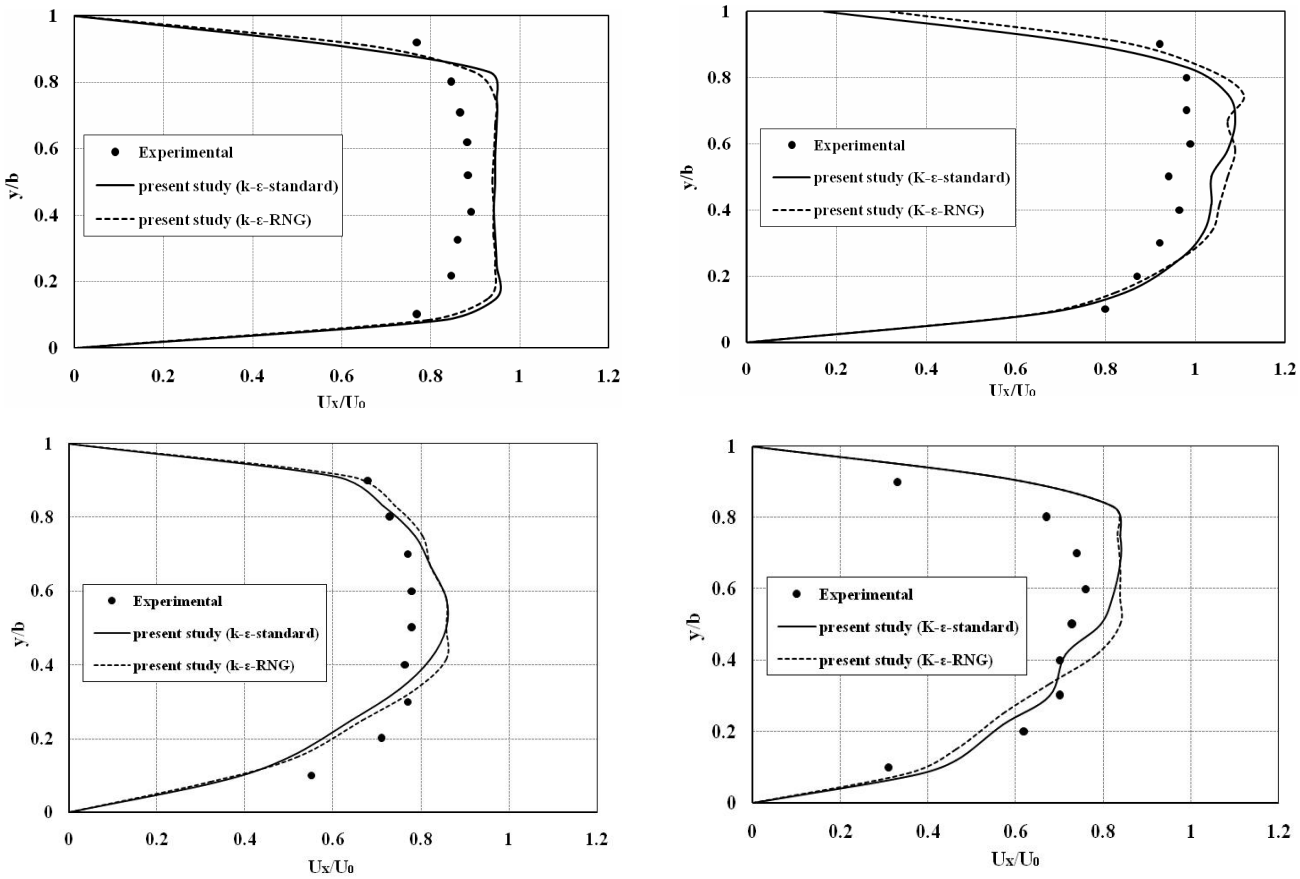

Figure 3. Evaluation of computational velocity profiles at different sections of the main channel using different turbulence models. (a) X^* = -4.65, (b) X^* = -0.5, (c) X^* = 0.5, and (d) X^* = 2.

According to Figure (3a), the velocity profile retains its expanded state before reaching the intake and when approaching the entrance, because of the suction flow, the velocity profiles will be deviated towards the intake channel and the maximum velocity will be deviated toward the intake entrance (section X* = -0.5) (Figure 3b).

The results showed that with flow entering to the intake, velocity resultant along the intake decreases and in the downstream wall of the entrance (section X* = 0.5), the maximum velocity will be distant from the inner wall of the main channel. The flow remaining in the main channel develops within the section after passing the intake entrance, but because of the effects of flow curved lines at the intake entrance, the maximum velocity will be deviated back towards the inner wall. The major cause of large values of the expected velocity to the experimental value is ignoring the effect of air stress in the numerical modeling.

Figure 4 also shows the dimensionless velocity profiles (U_y/U_0) near the water level, for different cross-sections of the intake channel. The numerical results obtained from Fluent Software are driven from the numerical study of Safarzadeh & Salehi Neishabouri (2004) and K-ε-Standard turbulence model is used for flow velocity profile distribution. The numerical results of Finite-Volume are also driven from numerical study of Goudarzizadeh et al (2010) in which K-ε-RNG turbulence model is used.

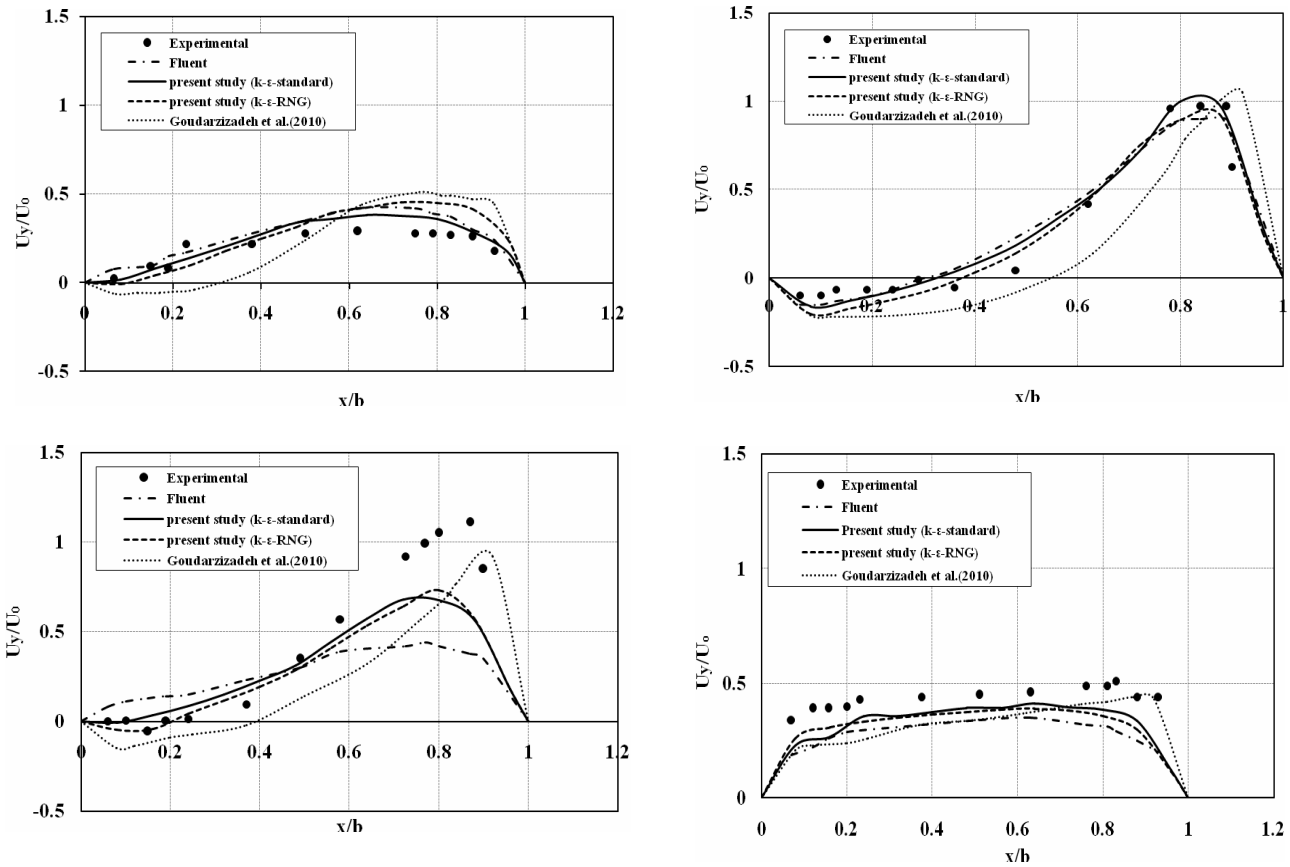

Figure 4. Evaluation of computational velocity profiles at different sections of the intake channel using different turbulence models. (a) $Y^* = 1$, (b) $Y^* = 2.5$, (c) $Y^* = 4$, and (d) $Y^* = 10$.

According to Figure 3 & 4, K-ε-standard turbulence model gains better results for estimation of velocity values from K-ε-RNG turbulence model, and well shows the positive and negative values in the two channels with a good agreement with experimental results. The cause of large values of the expected velocity to the experimental value is the effects of the secondary flow which lead to the movement of the maximum velocity to the water level low. Table 3 shows the mean error percentage obtained from the comparison of the numerical values resulted from present study and Fluent with experimental values at different sections of the main channel and intake.

Table 3

The mean percentage error obtained from the comparison of the numerical values of velocity profile at different sections of the two channels with the experimental values

Section	*X**				*Y**			
	-4.65	*-0.50*	*0.50*	*2.00*	*1.00*	*2.50*	*4.00*	*10.00*
Present Study (K-ε-Standard)	7.11	9.67	12.30	10.71	5.73	15.25	20.60	9.14
Present Study (K-ε-RNG)	7.42	10.72	13.47	11.42	11.20	20.76	22.02	10.05
Fluent		-			6.41	11.98	41.33	14.67

According to the good results obtained from the first section, the second section of this study investigates the averaged velocity profiles in depth at different sections of the main

channel and the intake of the experimental model of Shettar & Murthy (1996), using K-ε-standard turbulence model.

Characteristics of experimental model of Shettar & Murthy (1996). In the experimental study performed by Shettar & Murthy (1996), the lengths of main channel and intake are 6 m and 3 m respectively, which have 90 degrees. The flow rate entered into the main channel is 63 L/s, depth of flow is 0.25 m, width of both channels is 0.3 m and the Froude number of entrance flow is 0.54 (Figure 5b). Also, Figure (5a) shows view of computational domain meshing in the 90 degree intake.

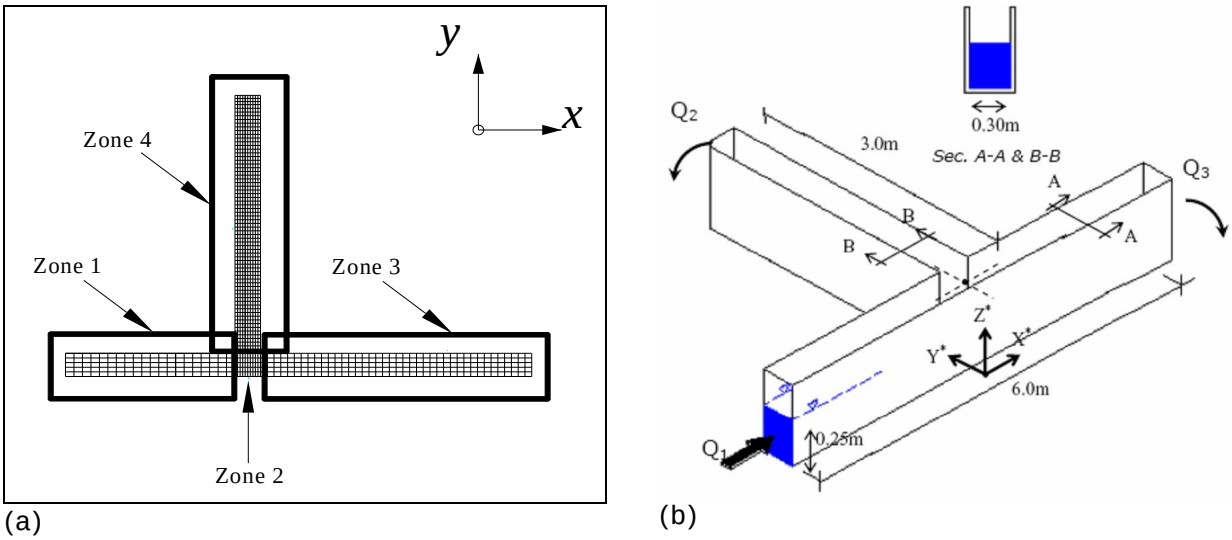

(a) (b)

Figure 5. Computational mesh which is used in simulation (a) and geometric characteristics of laboratory flume (b).

Meshing and boundary conditions of the computational domain. In the modeling of this section, wall boundary conditions are the same as the previous section, boundary condition in the channel entrance is considered constant velocity of 0.85 m/s. In the modeling, the ratio of diverted discharge (R) is considered 0.52, according to the amount considered in the experimental model. Table 4 shows the number and dimensions of cells in different areas of computational domain grid at x, y and z directions.

Table 4

The number and dimensions of cells in computational domain at different directions

	No. of cells at x direction	*No. of cells at y direction*	*No. of cells at z direction*	*Cell dimensions at x direction (mm)*	*Cell dimensions at y direction (mm)*	*Cell dimensions at z direction (mm)*
Zone 1	150.00	24.00	19.00	19.00	12.50	13.15
Zone 2	50.00	24.00	19.00	6.00	12.50	13.15
Zone 3	150.00	24.00	19.00	19.00	12.50	13.15
Zone 4	150.00	50.00	19.00	6.00	20.00	13.15

Evaluation of flow velocity profiles. In Figure 6, according to the experimental study, the averaged velocity profiles in depth at the x direction (U_x) are shown for different cross-sections of the main channel for entrance constant discharge of 63 L/s, the ratio of diverted discharge and the Froude number of entrance flow (Fr) 0.52 and 0.54,

respectively. The numerical results obtained from Fluent Software are driven from the numerical study of Shamloo & Pirzadeh (2008), in which K-ε-Standard turbulence model is used to examine flow velocity profile distribution.

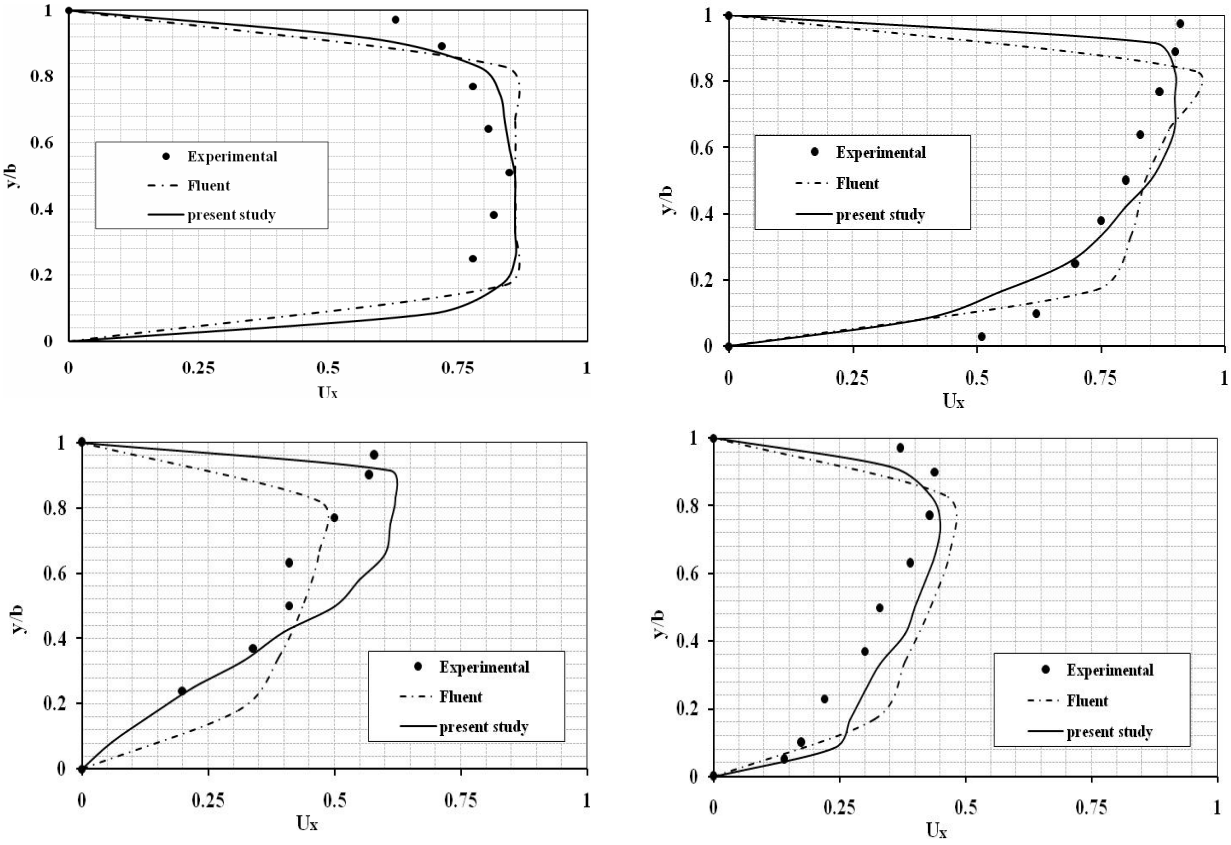

Figure 6. Evaluation of computational velocity profiles at different sections of the main channel. (a) X^* = -5.50, (b) X^* = -0.50, (c) X^* = 1.50, and (d) X^* = 7.

According to Figure 6a, similar to Figure 3a, the velocity profile retains its expanded state before reaching the intake entrance and when approaching the entrance, because of the suction flow applied by the intake, the velocity profiles will be deviated towards the intake. Also, the maximum velocity will be deviated toward the intake entrance (Figure 6b & 6c) and with flow entering to the intake, velocity resultant along the intake decreases.

Figure 7 shows the averaged velocity profiles in depths at the y direction (U_y) for different cross-sections of intake channel.

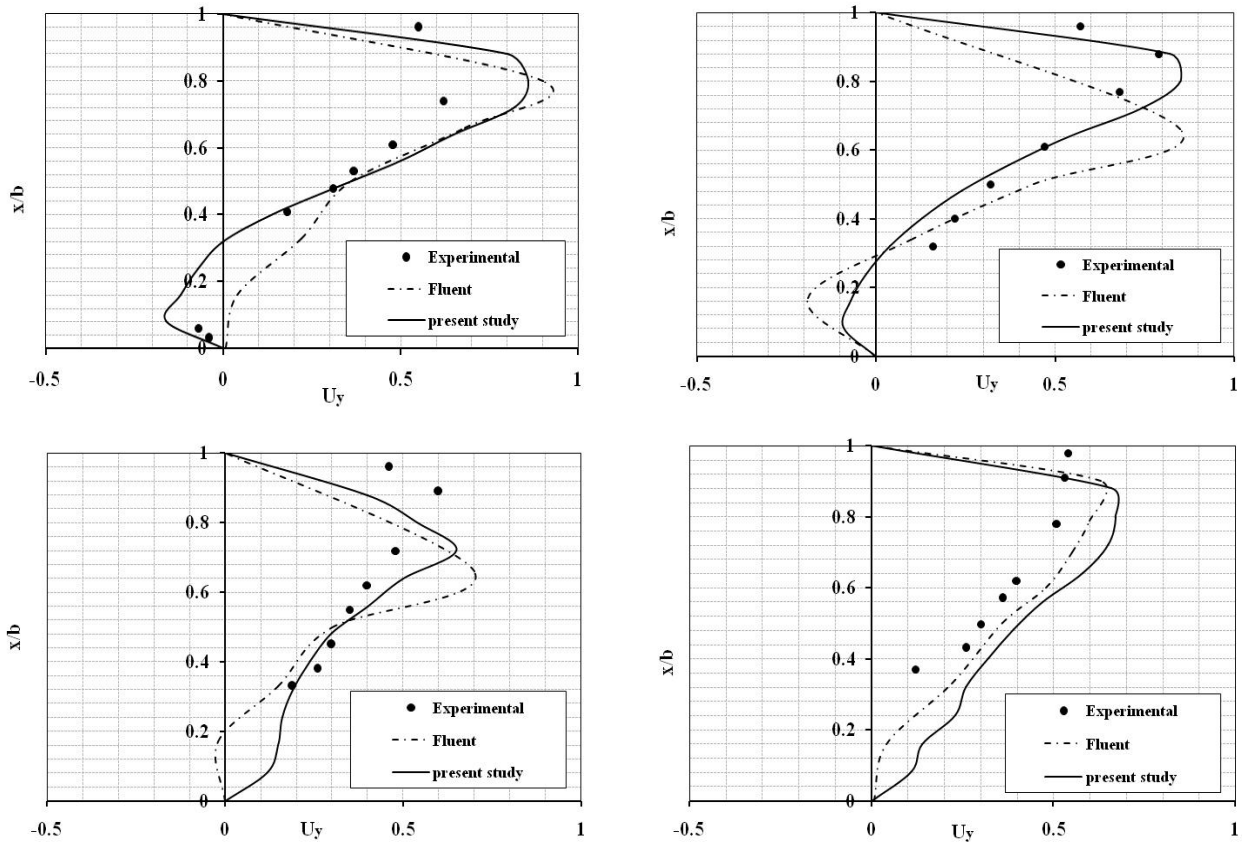

Figure 7. Evaluation of computational velocity profiles at different sections of the intake channel. (a) $Y^* = 0.65$, (b) $Y^* = 1.65$, (c) $Y^* = 2.65$, and (d) $Y^* = 3.65$.

As observed in Figures 6 & 7, accuracy of K-ε-standard turbulence model in the estimation of velocity at different sections of the intake and main channels is good and the predicted values in most sections are a little more than experimental values. Table 5 shows the mean error percentage obtained from the comparison of the numerical values resulted from present study and Fluent with experimental values at different sections of the main channel and intake.

Table 5

The mean error percentage obtained from the comparison of the numerical values of velocity profile at different sections of the two channels with the experimental values

Section	*X**				*Y**			
	-5.50	*-0.50*	*1.50*	*7.00*	*0.65*	*1.65*	*2.65*	*3.65*
Present study (K-ε-Standard)	4.47	4.67	10.15	4.65	11.46	7.66	3.55	14.33
Fluent	4.98	7.48	9.03	7.60	12.57	9.04	6.87	10.42

According to the errors percentage obtained from the comparison of the numerical values with the experimental results, the numerical values obtained from present study (FVM) at most sections, in good agreement with the experimental results, showed better results than the numerical results obtained from the Fluent numerical model, which indicated high ability of this numerical model in determining the velocity profile at different sections of the main channel and intake. In last section, according to the good results obtained from the above comparisons and ensuring high ability of this numerical model, the other parameters, such as shear stress and pressure distribution in the main channel and intake which have not been discussed in the experimental results, will be studied.

Figure 8 shows the graphical results (contours) of shear stress and pressure distribution in the main channel and intake for entrance discharge of 11 L/s, the ratio of diverted discharge and the Froude number of entrance flow are shown 0.31 and 0.13, respectively.

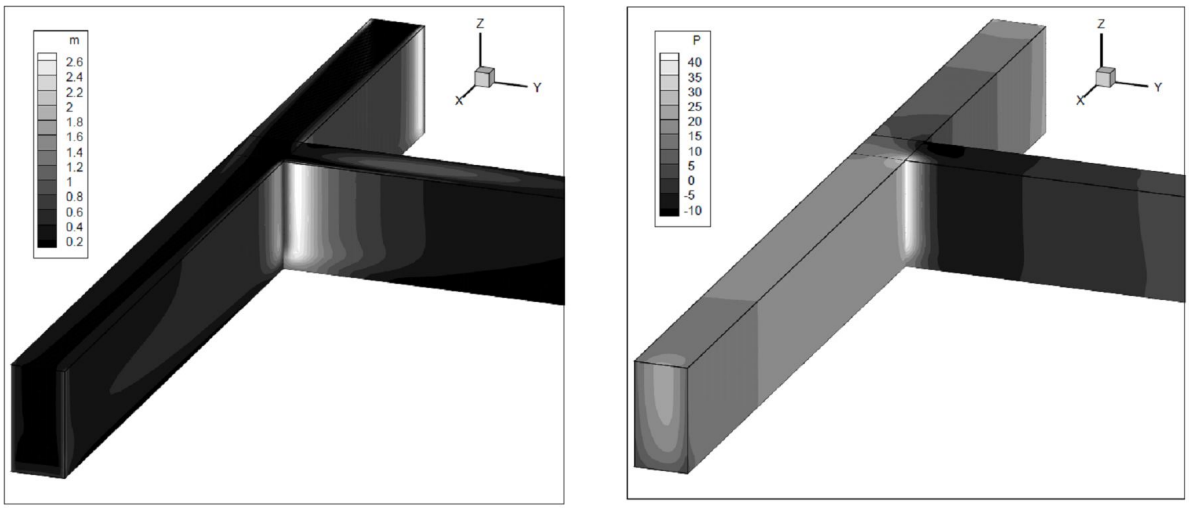

)a( )b(

Figure 8. Graphical results (contours) in the main channel and intake a) shear stress, b) pressure distribution.

According to Figure 8a, the maximum shear stress occurs at the entrance right wall of the intake, the amount of which is equal to 2.6 N/m^2. Given that wall corrosion will increase with increasing shear stress, it can be concluded that risk of corrosion in this area is greater than the other parts. Also, according to Figure 8b, entering the intake entrance, the pressure declines and when the flow passes through the intake entrance, stress distribution will become similar to the distribution before the intake. The maximum pressure is obtained on the right wall of the beginning of intake channel entrance, the amount of which is equal to 39.87 N/m^2.

Conclusions. The profile retains the velocity of its developed state before reaching the intake entrance and when approaching the entrance, because of the suction flow applied by the intake, the velocity profiles will be deviated towards the intake and the maximum velocity will be deviated toward the intake entrance (section X* = -0.5).

K-ε-standard turbulence model gain better results for estimation of velocity value from K-ε-RNG turbulence model, and its results estimate the positive and negative velocities in both channels with good agreement with the experimental results.

In both performed modeling, considering the error percentage obtained from the comparison of the numerical values with the experimental results, the numerical values obtained from present study in agreement with the experimental results, showed better results than the numerical results obtained from the Fluent numerical model, which indicated high ability of this numerical model in determining the velocity profile at different sections of the main channel and intake.

The maximum shear stress occurs at the entrance right wall of the intake, the amount of which is equal to 2.6 N/m^2. Given that erosion and corrosion will increase with increasing shear stress, it can be concluded that the risk of erosion and corrosion in this area is higher than in other areas.

References

Barkdoll B. D., Hagen B. L., Odgaard A. J., 1998 Experimental comparison of dividing open-channel with duct flow in T-junction. Journal of Hydraulic Engineering 124(1):92-95.

Chen H. B., Lian G. S., 1992 The numerical omputation of turbulent flow in T-junction. Journal of Hydrodynamics B No.3, pp. 50-58.
Goudarzizadeh R., Hedayat N., Mousavi Jahromi S. H., 2010 Three dimensional simulation of flow pattern at the lateral intake in straight path using finite volume method. World Academy of Science, Engineering and Technology 4(11):570-575.
Issa R. I., Oliveira P. J., 1994 Numerical prediction of phase separation in two-phase flow through T-Junctions. Computers and Fluids 23(2):347-372.
Hager W. H., 1987 Discussion of separation zone at open channel junction. Journal of Hydraulic Engineering 113(4):539-543.
Law S. W., Reynolds A. J., 1966 Dividing flow in an open channel. Journal of Hydraulic Engineering 92(2):207-231.
Neary V. S., Sotiropoulos F., Odgaard A. J., 1996 Three dimensional numerical model of lateral intake inflows. Journal of Hydraulic Engineering 125(2):126-140.
Neary V. S., Odgaard A. J., 1993 Three dimensional flow structure at open channel diversions. Journal of Hydraulic Engineering 119(11):1223-1230.
Neary V. S., Sotiropoulos F., Odgaard A. J., 1999 Three dimensional numerical model of lateral intake inflows. Journal of Hydraulic Engineering 125(2):126-140.
Olsen N. B. R., 2006 A three dimensional numerical model for simulation of sediment movements in water intakes with moltiblock option. Department of Hydraulic and Environmental Engineering, the Norwegian University of Science and Technology.
Popp M., Sallet D. W., 1983 Experimental investigation of one and two-phase flow through a tee junction. Proceedings of the International Conference on the Physical Modeling of Multi-Phase Flow, Coventry, England, 67–88.
Ramamurthy A. S., Junying Q., Diep V., 2007 Numerical and experimental study of dividing open-channels flows. Journal of Hydraulic Engineering 133(10):1135-1144.
Safarzadeh A., Salehi Nishabouri S. A. A., 2004 [Numerical modeling of flow 3D pattern in lateral intake]. 1th National Congress on Civil Engineering, Sanati Sharif University. [In Persian].
Shamloo H., Pirzadeh B., 2008 Investigation of characteristics of separation zones in T-junctions. Wseas Transactions on Mathematics 7(5):303-312.
Shettar A. S., Murthy K. K., 1996 A numerical study of division flow in open channels. Journal of Hydraulic Research 34(5):651-675.

Received: 19 May 2015. Accepted: 10 July 2015. Published online: 25 July 2015.
Authors:
Adel Asna Ashari, Islamic Azad University, Mahabad Branch, Young Researchers and Elite Club, Iran, Mahabad, Simbo St no. 334, e-mail: adel_asna a@yahoo.com
Edris Merufinia, Islamic Azad University, Mahabad Branch, Young Researchers and Elite Club, Iran, Mahabad, Simbo St no. 334, e-mail: edris.marufynia@yahoo.com
Ebrahim Nohani, Islamic Azad University, Dezful Branch, Department of Hydraulic Structures, Iran, Dezful, Koye Azadegan St. no. 313, e-mail: nohani_e@yahoo.com

How to cite this article:
Ashari A. A., Merufinia E., Nohani E., 2015 Numerical investigation of velocity profiles in the lateral intakes using finite-volume method and comparison with experimental results in water distribution networks. AACL Bioflux 8(4):544-555.